 doi:10.20944/preprints202207.0417.v1

Article

Present and Future Changes of Winter Cyclonic Activity in the Mediterranean-Black Sea Region in the 21st Century in CMIP6 models' Ensemble

Elena N. Voskresenskaya *, Veronika N. Maslova, Andrey S. Lubkov and Viktor Y. Zhuravskiy

Institute of Natural and Technical Systems; V.N.M. veronika_maslova@mail.ru; A.S.L. andrey-ls2015@yandex.ru; V.Y.Z. vectorj@mail.ru

* Correspondence: elena_voskr@mail.ru

Abstract: A better understanding of the expected future cyclonic activity, especially in the Mediterranean Basin in winter, is essential for developing scientifically based adaptation and mitigation methods to extreme precipitation and wind anomalies. The aim of this study is to analyze the change of winter cyclonic activity in the Mediterranean-Black Sea region, within the Atlantic–European region, at the beginning (as the recent historical period), middle and end of the 21st century. The projections are based on an ensemble of seven CMIP6 models, which showed the best consistency with NCEP/NCAR and ERA5 reanalysis, under the intermediate SSP2-4.5 and highest-emission SSP5-8.5 scenarios. The results show a consistent increase of the frequency of cyclones over Central Europe and the British Isles associated with the shift of cyclone tracks: norward from the Western Mediterranean region and southward from the Iceland Low. The latter leads to a decrease of the frequency in the north of the Atlantic–European region. At the same time, there is a reduction of the frequency of cyclones over the east of the Mediterranean Sea consistent with the decrease of cyclogenesis events. Area-averaged cyclone numbers in the Western and Eastern Mediterranean and the Black Sea subregions reduce to the end of the century under the highest-emission scenario, but not constantly and with a raise in the middle of the 21st century under both scenarios, which may be linked to the long-term multidecadal variability or regional features. In general, our study shows that the future winter cyclonic activity in the Mediterranean-Black Sea region responds unevenly to global climate changes, because regional and monthly features are important, as well as accounting for the long-term quasiperiodic variability.

Keywords: storm tracks; track density; cyclogenesis areas; climate variability and change; the North Atlantic Oscillation; the East Atlantic–West Russia pattern

1. Introduction

For historical, as well as future periods, cyclonic activity is the main mechanism of climate variability, including extremes, especially as for regional winter precipitation and wind anomalies of synoptic scale in the Mediterranean-Black Sea region. In a warmer atmosphere, cyclones may differ in their dynamic features (for example, location of trajectories) and thermodynamic processes (for example, changes in intensity). According to [1], cyclones are expected to become more diabatically driven. They tend to move slower, and their deepening rate becomes stronger [2]. All of the above can increase the frequency and intensity of adverse cyclone-related hydrometeorological and hydrological events, for example torrential precipitation, wind surges, severe river floods, landslides [3]. Considering these risks, the Mediterranean Basin is particularly vulnerable to climate change [4].

The physical processes responsible for cyclonic activity change in warmer climate have contrasting effect. On the one hand, an increase in sea surface temperatures and latent heat fluxes increase convection, therefore thermodynamic processes become more

 doi:10.20944/preprints202207.0417.v1

important. On the other hand, higher temperature increase in the upper troposphere increases atmospheric stability [3,4]. In addition, a warmer atmosphere can hold more moisture according to the Clausius–Clapeyron equation [3], which is expected to lead to increased water vapor transport [5] and cyclone-related precipitation [6,7], for example over the Western Atlantic and Mediterranean region [8]. The aqua-planet simulations in [1], with the uniform increase of the sea surface temperatures by 4 K, showed a 3.3 % decrease in the number of extratropical cyclones, no change in the intensity median but more stronger and more weaker storms, and an increase of precipitation associated with the strongest cyclones by up to 50%. Future increase in the frequency of cyclones associated with extreme precipitation over Europe was shown in [9].

There are three competing remote drivers of midlatitude atmospheric circulation change, mentioned in [10]: tropical and polar amplification of global warming and changes in the stratospheric vortex strength. The most important remote drivers of regional circulation over Europe are a high tropical amplification and a strengthening of the stratospheric vortex [10]. Tropical amplification is the broadening of the tropic / subtropical dry zone and the expansion of the Hadley Cell towards the poles [11]. It forces the poleward migration of jet streams [12] and storm tracks [13]. The North Atlantic jet stream shifts poleward in summer and extends eastward into Europe in winter [6]. Polar amplification results from the Arctic Sea ice loss, and may also affect meridional temperature gradients and storm tracks [14]. Strengthened stratospheric vortex is associated with a zonal wind anomaly that closely resembles the positive phase of the North Atlantic Oscillation [10]. The future increase in the positive phase of the North Atlantic Oscillation and associated northward migration of the mid-latitude cyclone tracks is mentioned in [11]. A poleward shift of storm tracks is projected as for the Northern Hemisphere in general [15], and for the North Atlantic in particular followed by the weakening of the Mediterranean storm track [16].

The influence of the modes of internal natural variability, such as the North Atlantic Oscillation (NAO), the East Atlantic/Western Russia (EAWR) patterns and others, on extratropical cyclones is recognized in the scientific community, for example [17–20], and not only in winter, but also in summer [21]. The natural variability was prevailing in the depth of the Northern Hemisphere winter extratropical cyclones before the industrial era [3]. In future, the influence of the simulated positive shift in the NAO index explains 10–50 % of the simulated trend of the cyclone decrease over the Western Mediterranean region [22].

Winter climatic anomalies in the Mediterranean-Black Sea region are driven mostly by the regional cyclonic activity associated with large-scale processes of global scale. In the terms of large-scale circulation, the projections of the North Atlantic storm tracks are the most important for the climate in the region. Further we consider the main features of cyclonic activity in future scenarios for the 21st century from the global to regional scale.

The researchers generally agree on the decrease in the frequency of cyclones at the end of the century generally over the Northern Hemisphere [23] and in the active storm track regions, particularly in the North Atlantic [24]. As for the intensity of cyclones, it is projected to increase in winter [25,26] or there will be an increase in the number of extreme cyclones in winter [23]. In the same season, cyclone-related heavy precipitation and strong winds are found to intensify [23,27].

As for the spatial pattern of the North Atlantic cyclonic activity, [27,28] showed future strengthening of the storm track around 50°N and the weakening of cyclone track density to the north over Scandinavia and to the south of the North Atlantic (stretching to the Mediterranean region). The pattern of winter cyclones over Europe was projected to become tripolar with an increased number of cyclones in Central Europe and a decreased number in the Norwegian and Mediterranean Seas [6].

Despite different identification and tracking methods of cyclones, as well as the biases and inconsistencies of the available models, and large spread among them, most projections for the Mediterranean region show the decrease in the number of winter cy-

 doi:10.20944/preprints202207.0417.v1

clones at the end of the 21st century [8,11,22,27,29,30]. This reduction continues the negative trends in the frequency of winter cyclones of the late 20th century [20,31–33]. In contrast, [2] showed that the number of cyclones in summer is projected to increase in the Mediterranean region almost by factor 2.

The change of cyclonic activity, and first of all cyclone tracks, leads to wetter or drier conditions in the Mediterranean region, as it was shown for example for its eastern part in [34]. While the intensity of each rainy event in a warmer atmosphere is locally important, the main reduction in precipitation observed in winter will be driven mainly by the decrease in the number of Mediterranean cyclones [30,35]. This overall reduction tends to be regionally compensated or amplified by the average precipitation generated by the individual cyclones in winter, which is projected to increase in the North Mediterranean (primarily associated with an increase in the atmospheric moisture content) and decrease in the East Mediterranean area (largely associated with a dynamical weakening of cyclones) [30].

The regional climate simulations show wetter winter conditions at the northern boundary [36] and central part [35] of the Mediterranean region, and drier conditions in the south-east of the basin, associated with the corresponding change of winter cyclone activity [35,36]. The strongest increase in aridity in the 21st century is expected for the south-eastern part of the Mediterranean region [35,37]. It is associated locally with the weakening of the specific synoptic circulation pattern called Cyprus Low [11,38]. Precipitation are projected to reduce also over the Iberian Peninsula due to the poleward shift of moisture corridors and associated atmospheric rivers [5] and reduction in cyclone occurrences [8].

Thus, the change of thermodynamic processes and atmospheric circulation under global warming conditions, taking into internal natural variability are expected to lead to the reduction of cyclonic activity, changes in current precipitation patterns and desertification в Mediterranean region. Nevertheless, the expected decrease of cyclonic activity in the Mediterranean region is not uniform in the different parts of region in different months and is likely associated with the shift of storm tracks. Not enough attention is also paid to the cyclonic activity change in the region at the middle of the century. The anomalies are estimated mainly relatively historical periods without taking into account new changed climatic norms.

Therefore, the aim of this study is to analyze the change in the winter cyclonic activity (frequency of cyclones, number of cyclogenesis events, number of cyclones, average cyclone tracks) in the Mediterranean-Black Sea region in the beginning (as the reference period), middle and end of the 21st century in the recent generation CMIP6 models' ensemble under the SSP2-4.5 and SSP5-8.5 scenarios. In some sense, we have addressed understanding of the time evolution (of multidecadal scale) of the climate change response in cyclonic activity at the middle and end of the 21st century relative to the reference period, which is provided with available reanalysis with assimilated observational data.

2. Data and Methods

The results of cyclonic activity projections are biased by many factors: accuracy and assumptions of the methods for cyclonic activity determining, spatial resolution and biases of the initial data, errors and discrepancies of the selected models, and the feasibility of emission scenarios.

Storm tracks can be identified using the Eulerian or Lagrangian approaches. The Eulerian method (or Laplacian-based methods) of storm activity, for example, is the identification of a storm track by a root mean square (RMS) of the filtered baric field (sea level pressure or geopotential height), e.g. [28], and the use of Laplacian of pressure to measure cyclone intensity. The Lagrangian method, which can provide more details (dynamic properties of cyclones, cyclogenesis areas), is based on cyclone identification and tracking algorithms applied mainly to the sea level pressure (SLP), geopotential

height or vorticity fields [25,29,39–48]. In this study we used the authors' cyclone identification and tracking method [49] based on the finding a minimum in the SLP field, which has been approved in [33] and is briefly described further in subsection 2.1.

To simulate cyclones in warmer climate in the 21st century, global circulation models (GSMs) are mainly used, either directly or as initial and lateral boundary conditions for downscaling in the Regional Climate Models (RCM), which are applied to obtain robust regional result, according to [11]. Higher-resolution models produce larger numbers of cyclones and storms [50], but this is not always useful for research purposes, for example, if the subject of the study refers to the manifestations of the large-scale atmospheric circulation in storm track changes. In particular, in contrast to the consensus on the reduction of cyclonic activity in the Mediterranean region in future, it was simulated in [51] using a 0.5° Regional Model (REMO), that the total number of cyclones in the Mediterranean region will increase, but at the expense of shallow, possibly thermal, cyclones. As for stronger winter cyclones, they were projected to decrease without significant changes of track properties and precipitation estimates along tracks, and that could indicate a northward shift of cyclone tracks [51].

Recently, some of the most popular global models are the families of models of the Coupled Model Intercomparison Project, phases 3, 5, 6 (CMIP3, CMIP5, CMIP6) [52–54]. The families of CMIP3, CMIP5, and CMIP6 models reproduce the consistent spatial structure of winter storm tracks in the North Atlantic – European region. At the same time, the most recent generation of CMIP6 models [54] is characterized by the lower multimodel mean biases in winter and are more sensitive in terms of larger amplitudes of the climate change and storm track change response [23,28,55]. Despite biases in the estimation of quantitative features, CMIP6 models show the improved atmospheric circulation over Europe relatively to the CMIP5 models [56], which is likely a result of increased horizontal resolution and improved model physics, according to [55].

There is a substantial spread among models in simulated future climate change. It emerges, on one side, from the pre-existing historical errors (systematic biases according to [Zappa et al., 2013a]) linked to the ocean state and its influence on large scale atmospheric baroclinicity (Priestley et al., 2021a,b). And on the other side, it arises from the differences in the projected atmospheric circulation change. For example, different CMIP5 GCMs are associated with high or low tropical amplification and weak or strong polar stratospheric vortex [57]. The driving GCMs further, with downscaling, amplify the uncertainties in regional models, which depend also on internal variability, model physics and the domain [35]. According to [58], the GCM boundary forcing is more important than RCM physics (internal RCM model processes), particularly in winter. Still, the spatial pattern of winter North Atlantic cyclones in CMIP5 projections seems to be only weakly affected by the biases of the models [6]. Some of the higher-atmospheric-resolution CMIP5 models (HadGEM2-ES, HadGEM2-CC,1 EC-EARTH, and MRI-CGCM3) have a better representation of both the number (storm-track position and tilt) and the intensity of North Atlantic cyclones than the majority of CMIP5 models, which have a storm track that is too zonal and shifted to the south [57]. In the RCM-based projections for the Mediterranean region, [35] showed that there are still important uncertainties (in the sign and magnitude) in changes of cyclone characteristics: the area of origin, seasonality, deepening rate of cyclones, associated precipitation and wind speed. Nevertheless, the uncertainties among models can be reduced by using model ensembles or multiple runs in the case of the same model.

We selected for the analysis all available CMIP6 models with a 6-hour time resolution, and with the availability of the recent historical period and two scenarios: SSP2-4.5 and SSP5-8.5. Thus, 8 CMIP6 models listed in Table 1 were used in the further analysis. Cyclones simulated in the each CMIP6 model were then compared to cyclones obtained using NCEP/NCAR and ERA5 reanalyses for a 15-year recent period of the beginning of the century (2000-2014).

Preprints (www.preprints.org) | NOT PEER-REVIEWED | Posted: 27 July 2022 doi:10.20944/preprints202207.0417.v1

Table 1. CMIP6 models analyzed in this study.

Model	Developer, country	Resolution
CMCC-CM2-SR5 [59]	Euro-Mediterranean Center on Climate Change, Italy	1.25×0.94
CMCC-ESM2 [60]		1.25×0.94
IPSL-CM6A-LR [61]	Institut Pierre Simon Laplace, France	2.5×1.27
MPI-ESM1-2-HR [62]	Max Planck Institute for Meteorology, Germany	0.94×0.93
MPI-ESM1-2-LR [63]		1.88×1.85
NorESM2-LM [64]	Norwegian Climate Centre, Norway	2.5×1.89
NorESM2-MM [64]		1.25×0.94
TaiESM1 [65]	Research Center for Environmental Changes, Academia Sinica, Taiwan	1.25×0.94

Simulations for the 21st century are conducted under different scenarios of economic growth. They assume various greenhouse gas concentration or emission trajectories, which lead to a range of additional incoming radiation per unit surface area (radiative forcing) and a range of global temperature increase. The greenhouse gas emissions trajectories were described in the Special Report on Emissions Scenarios (SRES) [66] and used in the IPCC's Third Assessment Report [67] and Fourth Assessment Report [68]. The families of the SRES scenarios (A1, A2, B1, B2) were replaced by the Representative Concentration Pathways (RCPs) in the IPCC Fifth Assessment Report [69] and by the Shared Socioeconomic Pathways (SSPs) in the IPCC Sixth Assessment Report [70].

The new generation CMIP6 models use the SSPs as scenarios of projected socio-economic global changes up to 2100. The most optimistic scenario among them is a SSP1-1.9 scenario with very low greenhouse gases (GHG) emissions (CO2 emissions cut to net zero around 2050), which is expected to lead to radiative forcing of 1.9 Wm-2 and global warming of 1°–1.8°C in 2081–2100. The most pessimistic SSP5-8.5 scenario with very high GHG emissions (CO2 emissions triple by 2075) is expected to lead to additional 8.5 Wm-2 and 4.4°C in 2081–2100 [70]. A moderate SSP2-4.5 scenario assumes intermediate GHG emissions (CO2 emissions around current levels until 2050, then falling but not reaching net zero by 2100). It is expected to lead to additional 4.5 Wm-2 and 2.7°C in 2081–2100. According to [71], the probability of SSP2-4.5 scenario is characterized as likely, while more pessimistic and optimistic scenarios as unlikely. More optimistic scenarios assume the implementation of international agreements on emission reductions. They are unreachable because of the lack of an effective legal regulation of control over anthropogenic emissions (greenhouse gases and aerosols) at the national levels of the main countries-emitters [72,73].

In this study, we used two SSPs. One of them is the SSP2-4.5 scenario which is the "middle-of-the-road" experiment in CMIP6. Additionally, we considered the SSP5-8.5 scenario as the highest-emission and the worst (no-policy) case.

2.1. Cyclone identification and tracking method

Cyclones were identified using 6-hourly sea level pressure fields (SLP) of the eight CMIP6 models, NCEP/NCAR [74] and ERA5 [75] reanalyses over the Atlantic-European region (20°W-45°E, 30°N-80°N).

The search for the low pressure center in a regular grid was as follows: if SLP increased in 4 directions upon sequential consideration of each grid point, then the starting point was identified as a minimum of the pressure field. To estimate the size of a baric formation, the SLP was estimated at each next grid point in 4 directions. If SLP began to decrease in one of the directions, then the value of the previous point was considered to be the last closed isobar of a cyclone. The selected models and reanalyses have different spatial resolution, and therefore it would be reasonable to introduce the minimum cyclone size, taking into account the coarsest spatial grid. In this work, all cyclones with the size less than 560 km were not taken into account.

Preprints (www.preprints.org) | NOT PEER-REVIEWED | Posted: 27 July 2022 doi:10.20944/preprints202207.0417.v1

After identification of the centers of low atmospheric pressure, the tracking of cyclones was carried out. The average maximum speed of an extratropical cyclone in the middle latitudes is 80-90 km/h [76]. Thus, a cyclone can move more than 2000 km per day. In many studies, daily data are used to identify and track cyclones, however, such a time scale can lead to the error of combining an occluded cyclone with a young one located within a radius of 2000 km.

The use of 6-hour data makes it possible to reduce the estimated radius of the location of cyclone at the next time step by a factor of 4, and, therefore, to avoid the problem of incorrect combination of cyclones. In this study, the two centers were linked if the other low-pressure center was found within a radius of 600 km at the next or previous 6-hour time step. If several such centers were found within the search radius, the nearest low-pressure center was selected.

There is a probability of occurrence of false baric lows associated with the influence of the relief on the SLP field. To avoid this problem, we applied a condition for the cyclone lifetime of at least 48 hours (8 time steps) and for the distance traveled of at least 1000 km, by analogy with [23].

The frequency of cyclones is defined as the number of 6-hour periods, when a cyclone center was observed.

As a result, the datasets of cyclones over the Atlantic-European region were obtained for the recent historical period of the beginning of the century (2000-2014) using eight CMIP6 models, NCEP/NCAR and ERA5 reanalyses, as well as for two future 15-year periods at the middle (2043-2057) and end (2086-2100) of the 21st century using the selected CMIP6 models under SSP2-4.5 and SSP5-8.5 scenarios.

2.2. Model scaling and comparison

All the calculated datasets have different spatial resolution, since no preliminary scaling of the SLP fields was performed. At the same time, the use of any interpolation procedure is undesirable, because as a result, the number of cyclones for high-resolution models will decrease. To solve this problem, all fields were scaled to a spatial resolution of 2.5°×2.5° as follows. The Atlantic-European region was divided into sectors sized 2.5°×2.5°. All centers of cyclones were summed (X) in each sector (i, j). To account for the contribution of a different number of points, each sector was weighted (X') according to the equation (1):

$$X'_{i,j} = X_{i,j} \frac{M}{m \cdot N}, \quad (1)$$

where M is a number of initial resolution points in the region, N is a number of sectors of normalized resolution (in our case it is 475 sectors in 2.5°×2.5° resolusion), m is the number of model or reanalysis points within the sector.

The quality of reproduction of cyclones in the CMIP6 models was assessed by comparison with cyclones obtained using NCEP/NCAR and ERA5 reanalyses over a 15-year recent historical period (2000-2014). The analysis was carried out on the basis of the frequency fields of cyclones normalized to a single spatial resolution. The comparison criteria were as follows:

- The Pearson's linear correlation coefficient according to equasion (2):

$$r = \frac{cov(x_i\, y_i)}{\sigma_x \sigma_y}, \quad (2)$$

where samples x and y are the spatial fields of the CMIP6 model and reanalysis converted into a vector, σ_x and σ_y are the standard deviations of samples x and y;

- The root mean square error of the model relative to reanalysis (RMSE) according to equasion (3):

$$RMSE = \sqrt{\frac{\sum(x_i - y_i)^2}{n}}, \quad (3)$$

Preprints (www.preprints.org) | NOT PEER-REVIEWED | Posted: 27 July 2022 doi:10.20944/preprints202207.0417.v1

where n is a number of grid points. Significant correlation is 0.16 at probability level p=0.001 (for 567 points of a regular grid).

2.3. Subregions for boxplots

Area-averaged winter cyclone numbers were calculated and represented as boxplots (see Fig. 7) at the beginning, middle and end of the 21st century for the three subregions of the Mediterranean Basin, as it is shown in Figure 1. Subregions were bounded in accordance with the main cyclogenesis areas of the Mediterranean Basin in the CMIP6 model ensemble (e.g., see Fig. 4). For each subregion, three cyclone numbers were considered: frequency of cyclones, number of cyclones and cyclogenesis events.

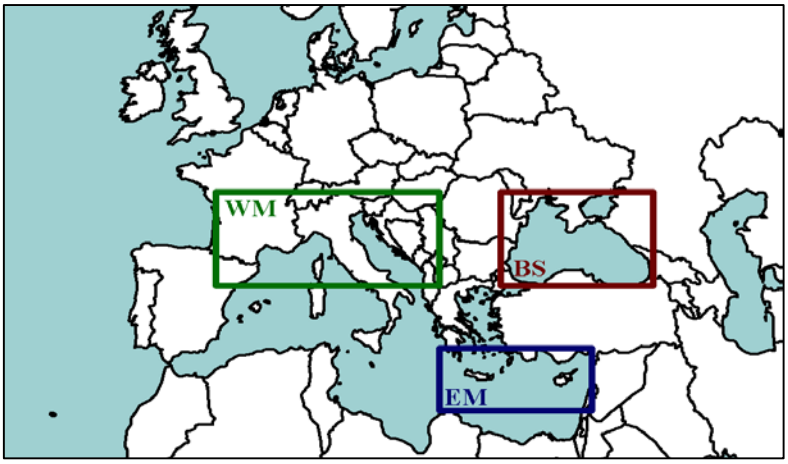

Figure 1. Boundaries of the subregions for calculating boxplots: Western Mediterranean (WM, 1°W-21°E, 41°N-47°N), Eastern Mediterranean (EM, 21°W-36°E, 33°N-37°N) and Black Sea (BS, 27°W-42°E, 41°N-47°N).

3. Results

3.1. Comparison with reanalyses

Cyclones were calculated over the Atlantic-European region for the recent historical period (2000-2014) in the CMIP6 models (from Table 1) and compared with those obtained using NCEP/NCAR and ERA5 reanalyzes. The monthly comparison results are shown in Tables 2 and 3 for the cold period from October to March. For the other months, the comparison results are considerably worse than those shown in these tables. The best consistency is found for the months from November to February. In general, all models showed approximately the same level of correlation and root mean square error (RMSE) for these months, except for the MPI-ESM1-2-HR model. The correlation with ERA5 (NCEP/NCAR) reanalysis is in the range 0.26-0.52 (0.18-0.4), and RMSE is in the range 4.9-6.7 (4.6-7.8), respectively. Model MPI-ESM1-2-HR has similar values of the correlation coefficients, but the RMSE values are almost twice as high as those of the rest of the models. The model MPI-ESM1-2-HR was excluded from the ensemble mostly because of the high RMSEs, especially with NCEP/NCAR reanalysis, and lower consistency with ERA5 reanalysis. The ensemble included 7 remaining models, which were characterized by the best correlation and the lowest root mean square error.

The ensemble values were calculated as the average cyclone numbers in each point of the normalized 2.5°×2.5° grid and summed up for each 15-year period. The results of the comparison (Tables 2, 3) led us to the decision to focus the analysis on the conventional winter season and winter months from December to February.

Table 2. Spatial linear correlation coefficient (r) and root mean square error (*RMSE*) between the frequency of cyclones over the Atlantic-European region in the CMIP6 models and NCEP/NCAR

Preprints (www.preprints.org) | NOT PEER-REVIEWED | Posted: 27 July 2022 doi:10.20944/preprints202207.0417.v1

reanalysis in the 2000–2014 period. The highest (for *r*) and lowest (for *RMSE*) 30% values of the entire range of the comparison parameter (for both reanalyses and all 12 months) are marked in bold.

CMIP6 model	Parameter	October	November	December	January	February	March
CMCC-CM2-SR5	*r*	0.14	**0.34**	0.26	**0.38**	0.32	0.21
	RMSE	7.03	6.36	6.52	6.76	**5.75**	6.39
CMCC-ESM2	*r*	0.19	0.24	0.31	**0.38**	0.21	0.21
	RMSE	7.2	7.02	6.19	6.21	6.23	6.51
IPSL-CM6A-LR	*r*	0.28	0.14	0.32	0.26	0.28	**0.33**
	RMSE	**5.48**	6.18	**5.44**	6.08	**4.97**	6.02
MPI-ESM1-2-HR	*r*	0.04	0.21	0.29	**0.44**	0.29	0.2
	RMSE	14.71	9.19	10.04	9.55	11.28	13.08
MPI-ESM1-2-LR	*r*	0.32	**0.34**	**0.4**	**0.37**	**0.45**	**0.33**
	RMSE	**4.61**	5.93	**5.6**	**5.82**	**4.57**	**5.18**
NorESM2-LM	*r*	**0.34**	0.27	0.22	0.18	**0.34**	0.2
	RMSE	**4.42**	**5.01**	**5.46**	6.11	**4.72**	**4.9**
NorESM2-LM	*r*	0.22	0.19	**0.31**	**0.35**	0.31	0.18
	RMSE	7.74	8.23	7.81	8.38	7.48	8.09
TaiESM1	*r*	0.18	0.3	**0.33**	**0.35**	0.17	0.16
	RMSE	7.57	6.46	6.02	7.01	6.54	7.22

Table 3. Spatial linear correlation coefficient (*r*) and root mean square error (*RMSE*) between the frequency of cyclones over the Atlantic-European region in the CMIP6 models and ERA5 reanalysis in the 2000–2014 period. The highest (for *r*) and lowest (for *RMSE*) 30% values of the entire range of the comparison parameter (for both reanalyses and all 12 months) are marked in bold.

CMIP6 model	Parameter	October	November	December	January	February	March
CMCC-CM2-SR5	*r*	0.19	**0.44**	**0.45**	**0.41**	**0.35**	0.2
	RMSE	6.95	**5.79**	**5.51**	6.09	**5.8**	6.88
CMCC-ESM2	*r*	0.26	**0.39**	**0.47**	**0.46**	**0.36**	0.29
	RMSE	6.78	6.08	**5.28**	**5.41**	**5.7**	6.13
IPSL-CM6A-LR	*r*	0.33	0.27	**0.44**	**0.37**	0.28	**0.35**
	RMSE	**5.58**	**5.88**	**4.94**	**5.33**	**5.54**	5.93
MPI-ESM1-2-HR	*r*	0.1	0.23	0.23	**0.35**	0.19	0.11
	RMSE	14.71	9.19	10.04	9.55	11.28	13.08
MPI-ESM1-2-LR	*r*	0.31	0.22	0.33	0.32	0.26	0.31
	RMSE	**5.62**	6.57	**5.81**	6.01	6.01	**5.9**
NorESM2-LM	*r*	**0.36**	**0.42**	**0.41**	**0.38**	**0.34**	0.29
	RMSE	**5.6**	**5.24**	**5.01**	**5.53**	**5.68**	**5.89**
NorESM2-LM	*r*	0.32	**0.39**	**0.51**	**0.52**	**0.42**	0.27
	RMSE	6.81	6.83	6.28	6.72	6.41	7.41
TaiESM1	*r*	0.21	**0.42**	**0.46**	**0.47**	**0.36**	0.21
	RMSE	7.3	**5.74**	**5.17**	**5.8**	**5.82**	6.99

3.2. Ensemble fields

 doi:10.20944/preprints202207.0417.v1

Figure 2 shows the frequency of the winter (DJF) cyclones and the number of cyclogenesis events in the recent historical period (2000–2014) over the Atlantic-European region according to NCEP/NCAR and ERA5 reanalyses, and CMIP6 ensemble. The spatial patterns of the frequency (Fig. 2a, c, e) are similar, and their differences in the representation of details and cyclone numbers can be attributed to the resolution of the models. As for the number of cyclogenesis events (Fig. 2b, d, f), there is less similarity in the spatial patterns, but the location of the main centers is roughly consistent. In general, the agreement of fields of the frequency of cyclones and the number of cyclogenesis events looks better between ERA5 reanalysis and CMIP6 ensemble, which is also indicated by the quantitative estimates in Table 3 compared to Table 2.

For the CMIP6 ensemble, the maximum winter frequency of cyclones in the Mediterranean Basin in the recent historical period (Fig. 2e) is over half of the water area along the northeastern coast of the Mediterranean Sea approximately from Corsica to Cyprus with an increase to the east. Other maxima are over the north-east of the North Atlantic (to the south of Iceland, over the North Sea, off the coast of the Norwegian Sea) and also over the continent and inland seas (the Baltic Sea, over the Black Sea and northward to the White Sea). The month of the highest winter frequency of cyclones is January, and the lowest frequency is in February (not shown). The main cyclogenesis areas according to the CMIP6 ensemble (Fig. 2f) are located along the northern Mediterranean coast from the Gulf of Lyon to the west of the Black Sea, over the Baltic Sea and North Sea, over Iceland and partly over the Norwegian Sea. These cyclogenesis areas are consistent with those in studied, e.g., in [77].

Figures 3 and 4 show the frequency of the winter cyclones and the number of cyclogenesis events over the Atlantic-European region projected for the middle (2043–2057) and end (2086–2100) of the 21st century in the in the CMIP6 ensemble under the SSP2-4.5 and SSP5-8.5 scenarios. Almost all areas of the maximum cyclone numbers shrink and become noticeably weaker to the end of the century, except for that over the north-east North Atlantic. For the Mediterranean Sea, the largest decrease is in January (not shown). The SSP5-8.5 scenario is characterized by lower values of cyclone numbers than the SSP2-4.5 scenario, which is consistent with studies of the future synoptic circulation for the regions from global [15] to local [38].

To characterize these differences, Figure 5 shows absolute anomalies of the frequency of winter cyclones in the middle (2043–2057) and end (2086–2100) of the 21st century relatively the recent historical period of the beginning of the century (2000–2014). The patterns of anomalies look very much alike for different scenarios for the same period, but with larger differences for the SSP5-8.5 scenario than for the SSP2-4.5 scenario in the areas of the greatest anomalies. Similar estimates for the zonally averaged storm track over the Northern Hemisphere at the end of the 21st under the RCP8.5 scenario are almost twice as large as those projected for the mid-21st century [15]. In the spatial structure of anomalies, there is a consistent (among models) increase over Central Europe and the British Isles and decrease over the east of the Mediterranean Sea and in the north of the region (Iceland, North Sea, White Sea).

Preprints (www.preprints.org) | NOT PEER-REVIEWED | Posted: 27 July 2022 doi:10.20944/preprints202207.0417.v1

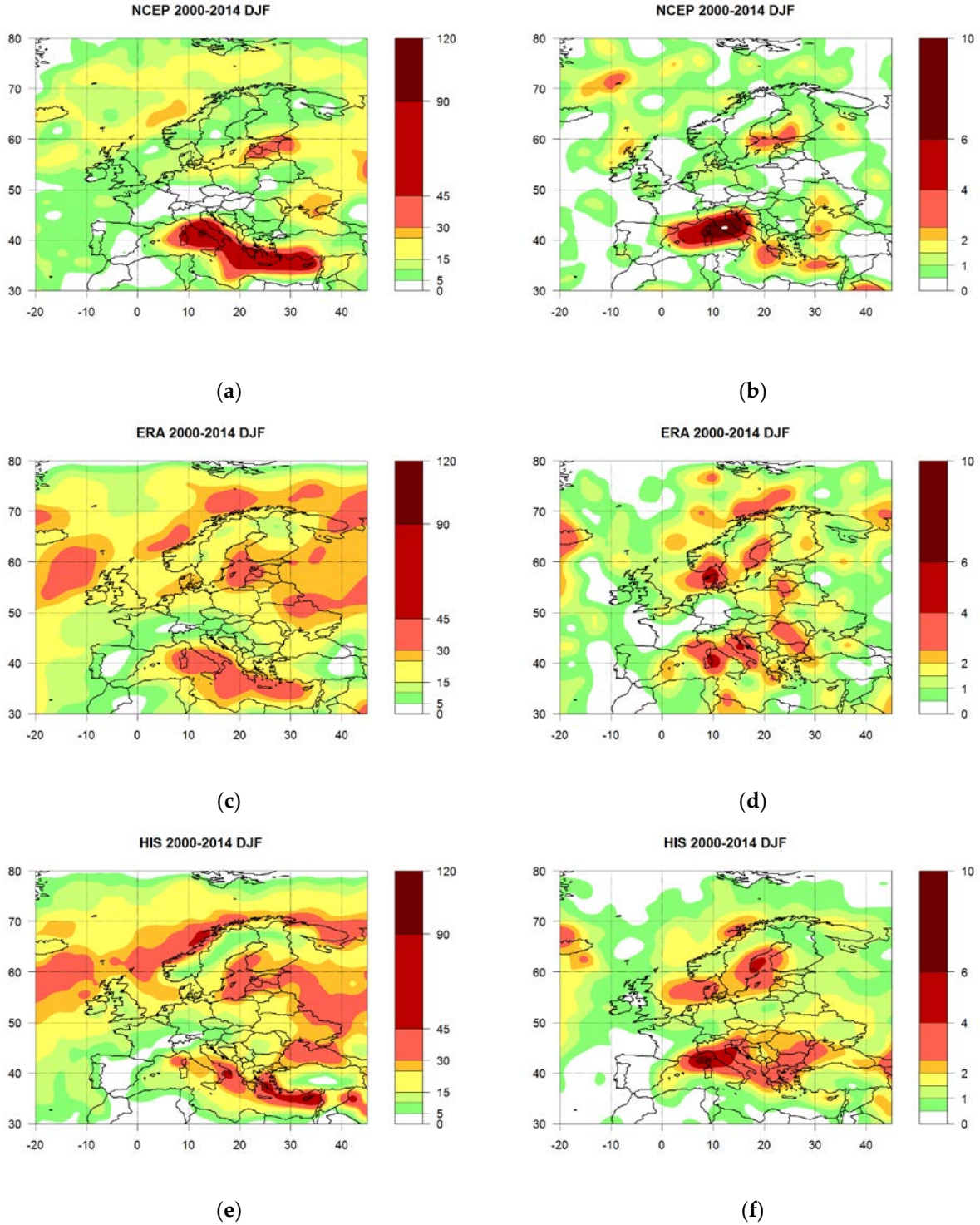

Figure 2. Winter cyclone numbers in the recent historical (HIS, 2000–2014) period: (**a**, **c**, **e**) Frequncy; (**b**, **d**, **f**) Cyclogenesis events; based on: (**a**, **b**) NCEP/NCAR reanalysis; (**c**, **d**) ERA5 reanalysis; (**e**, **f**) CMIP6 ensemble.

Preprints (www.preprints.org) | NOT PEER-REVIEWED | Posted: 27 July 2022 doi:10.20944/preprints202207.0417.v1

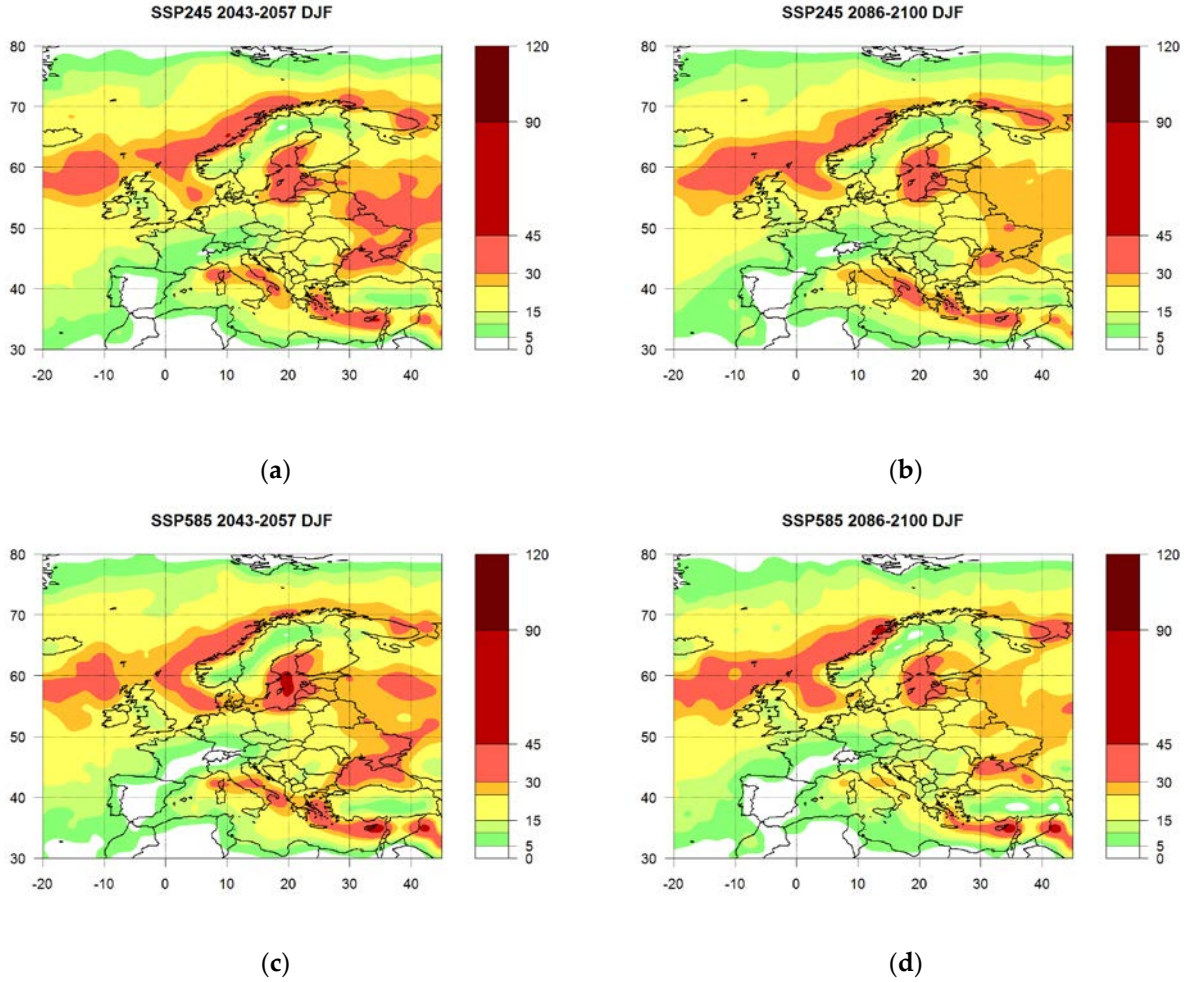

Figure 3. Frequency of winter cyclones according to the ensemble of the CMIP6 models: (**a**, **c**) At the middle of the 21st century; (**b**, **d**) At the end of the 21st century; (**a**, **b**) Under the SSP2-4.5 scenario; (**c**, **d**) Under the SSP5-8.5 scenario.

Preprints (www.preprints.org) | NOT PEER-REVIEWED | Posted: 27 July 2022 doi:10.20944/preprints202207.0417.v1

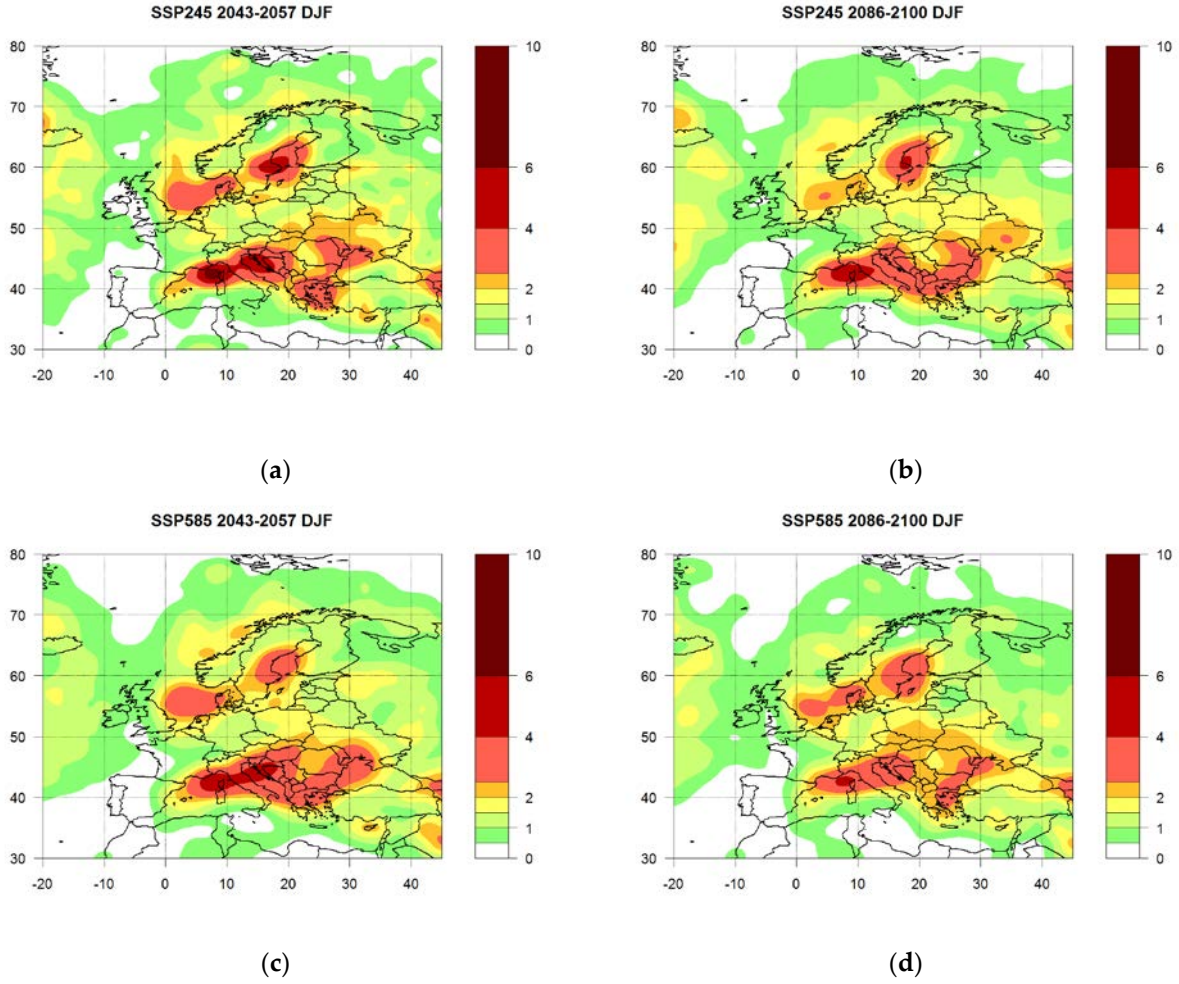

Figure 4. Number of winter cyclogenesis events according to the ensemble of the CMIP6 models: (**a**, **c**) At the middle of the 21st century; (**b**, **d**) At the end of the 21st century; (**a**, **b**) Under the SSP2-4.5 scenario; (**c**, **d**) Under the SSP5-8.5 scenario.

This spatial structure is consistent with the results of simulations of cyclonic activity for the 21st century in [6,23,36]. On the basis of regional climate model RegCM under the IPCC A2 and B2 emission scenarios, [36] showed higher cyclone frequency in the end of the century under the A2 and B2 scenarios over the North Sea, Central Europe and to the west of the British Isles, and lower frequency over Cyprus (under the B2 scenario) and Eastern Mediterranean (under the A2 scenario). Using CMIP5 models under the RCP4.5 emission scenario, [6] showed in that the winter (DJF) response is characterized by a tripolar pattern over Europe, with an increase in the number of cyclones in Central Europe and a decreased number in the Norwegian and Mediterranean Seas in the result of the eastward extension of the Atlantic storm track into Europe. Using CMIP6 models featured by the SSP2-4.5 and SSP5-8.5 scenarios, [23] also showed an extension of the North Atlantic storm track into Europe, an increase in the track density over NW Europe and particularly the British Isles, and a decrease in activity over the Mediterranean region, south-western Europe and Norwegian Sea. This tripolar pattern is consistent with the dipole pattern found in [5], who showed a significant increase in the frequency of dry weather types over the Iberia and an opposite signal over the British Isles associated with a stronger north–south dipole in terms of pressure and precipitation distributions, enhancing the transport toward central Europe rather than to Iberia [5]. An increase in most models of the future number of intense cyclones in winter over the British Isles and Northeast Atlantic was mentioned in the review by [25], while the number of all extra-

Preprints (www.preprints.org) | NOT PEER-REVIEWED | Posted: 27 July 2022 doi:10.20944/preprints202207.0417.v1

tropical cyclones will be reduced under anthropogenic climate change conditions [25]. A review [26] summarizes, that future scenarios to the end of the 21st century indicate mostly an increase in winter storm intensity over the Western Europe.

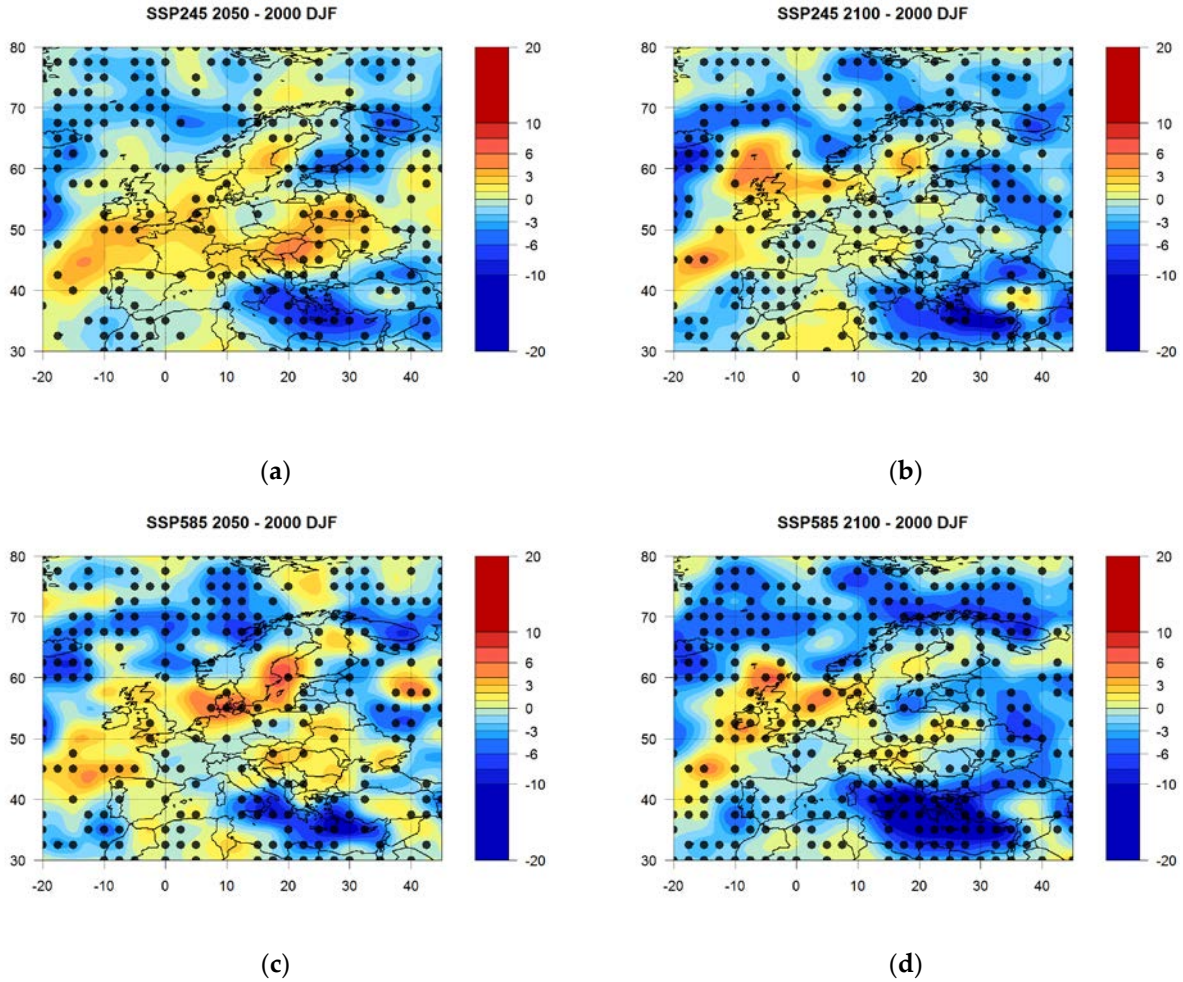

Figure 5. Absolute anomalies of the frequency of winter cyclones relative to the recent historical period (2000–2014) of the beginning of the century: (**a**, **c**) At the middle of the 21st century; (**b**, **d**) At the end of the 21st century; (**a**, **b**) Under the SSP2-4.5 scenario; (**c**, **d**) Under the SSP5-8.5 scenario. Stippling indicates where 70% of the models agree on the sign of change.

Figure 6 shows monthly winter anomalies which are characterized by regional features. The greatest negative anomalies are observed in January for both scenarios, especially in the Eastern Mediterranean region, and the greatest positive ones are in December at about 50°–60° N, including the western shores of Europe, while in February the anomalies are mostly less pronounced.

As well as for the winter season anomalies (Fig. 5), for the anomalies of the winter months (Fig. 6) one can observe the similarity of the spatial patterns for the different scenarios in the same period, especially for December and January. At the same time, the SSP5-8.5 scenario is characterized by the prevalence of the negative anomalies of the frequency of cyclones for the Atlantic-European region in general, but with regional and monthly features. Thus, under the SSP5-8.5 scenario, along with negative anomalies, there is also an increase in positive anomalies in different parts of Europe in December in the middle of the century (Fig. 6a, d) and in February at the end of the century (Fig. 6i, l), and in January, in the middle of the century, negative anomalies in the eastern Mediterranean Sea are less pronounced than under the SSP2-4.5 scenario.

Preprints (www.preprints.org) | NOT PEER-REVIEWED | Posted: 27 July 2022 doi:10.20944/preprints202207.0417.v1

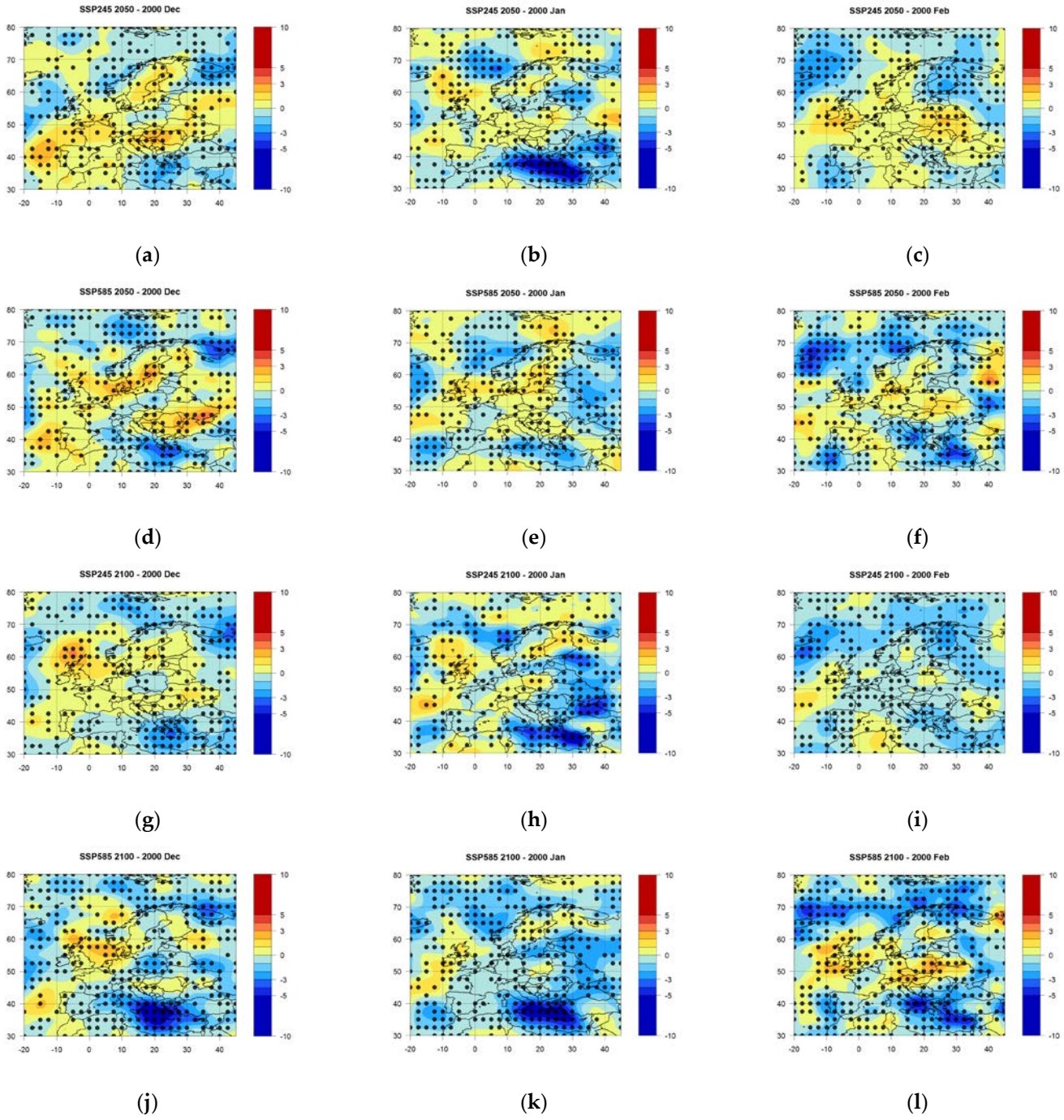

Figure 6. Absolute anomalies of the frequency of cyclones relative to the recent historical period (2000–2014) of the beginning of the century in December (left column), January (central column) and February (right column): (**a–f**) At the middle of the 21st century; (**g–l**) At the end of the 21st century; (**a–c**, **g–i**) Under the SSP2-4.5 scenario; (**d–f**, **j–l**) Under the SSP5-8.5 scenario. Stippling indicates where 70% of the models agree on the sign of change.

3.3. Area-averaged cyclone numbers

Figure 7 shows area-averaged winter cyclone numbers (frequency of cyclones, number of cyclones and number of cyclogenesis event) at the beginning, middle and end of the 21st century for three subregions: the Western Mediterranean, Eastern Mediterranean and Black Sea. For all subregions, under the considered scenarios, there is no continuous reduction of cyclone numbers in the 21st century as it was the case, for example, for the total number of Northern Hemisphere winter extratropical cyclones in the CMIP6

Preprints (www.preprints.org) | NOT PEER-REVIEWED | Posted: 27 July 2022 doi:10.20944/preprints202207.0417.v1

models in [23] and for the zonally averaged midlatitude storm track changes in the CMIP5 models in [15]. Nevertheless, the largest drop of the median of all boxplots in Figure 7 is expected for the end of the century under the SSP5-8.5 scenario, while cyclone numbers (measured by the median of boxplots) in the middle of the century under the same scenario are the highest among climate change responses.

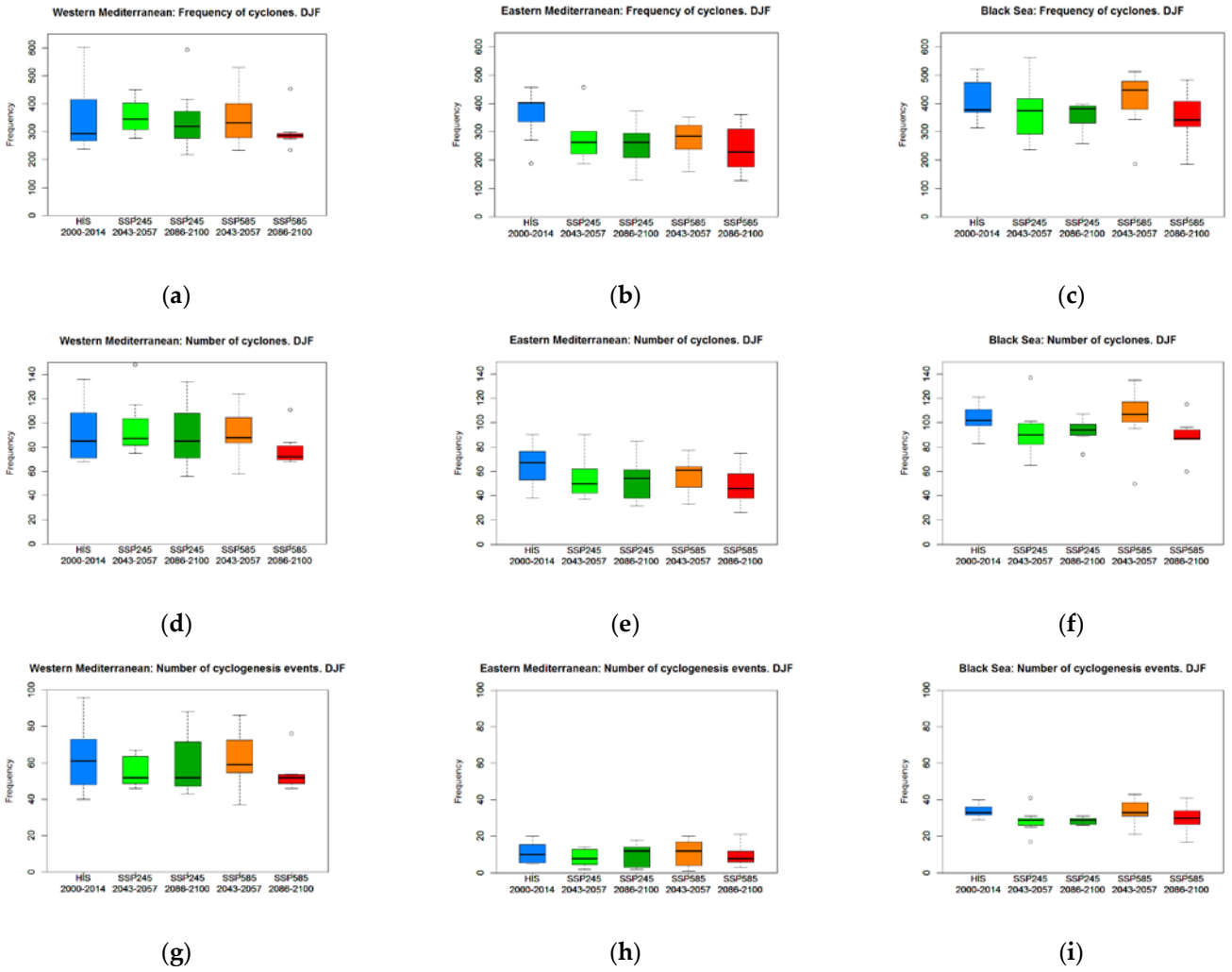

Figure 7. Boxplots of the area-averaged winter cyclone numbers: (**a**, **b**, **c**) Frequency of cyclones; (**d**, **e**, **f**) Number of cyclones; (**g**, **h**, **i**) Number of cyclogenesis events; for the subregions (see Fig. 1): (**a**, **d**, **g**) Western Mediterranean; (**b**, **e**, **h**) Eastern Mediterranean; (**c**, **f**, **i**) Black Sea; at the recent historical period (*blue*), middle of the century under the SSP2-4.5 scenario (*light green*), end of the century under the SSP2-4.5 scenario (*green*), middle of the century under the SSP5-8.5 scenario (*orange*), and end of the century under the SSP5-8.5 scenario (*red*). The black line in the boxes is the median, the boxes range is 25th–75th percentiles, the whiskers range is 5th–95th percentiles, the white dots mark the outliers.

Under the SSP2-4.5 scenario, in the Western Mediterranean subregion, cyclone numbers (frequncy and cyclogenesis events) are projected to increase in the middle of the century and to fall by the end of the century to the level of recent cyclone numbers of the beginning of the century, but not at the expense of cyclogenesis events within this subregion, which are expected to decrease in the middle of the century and not to change (in the boxplot median of the ensemble of CMIP6 models) by the end of the century. An expected increase in cyclone numbers in the Western Mediterranean subregion in the middle of the century may be associated with an increase in cyclogenesis events over the Balearic Sea (Fig. 4a,b). This result is consistent with the result for strong cyclone systems

 doi:10.20944/preprints202207.0417.v1

(<995 hPa) in winter over the north-western Mediterranean subregion in [51], who showed that cyclone numbers in a Regional Model (REMO) under the (IPCC SRES) B2 scenario are higher in the mid-century (2030–2064) and lower in the end of the century (2065–2099) than in the beginning (1995–2029) of the period.

In the Eastern Mediterranean and the Black Sea subregions, cyclone numbers under the SSP2-4.5 scenario are expected to decrease in the middle of the century (with the largest drop in the frequency of cyclones for the Eastern Mediterranean subregion in Fig. 7e), and then stay at the same level to the end of the century. We obtained milder area-averaged responses for the whole Eastern Mediterranean subregion, than it was found using CMIP5 models in [38] for the local Cyprus Low circulation type, who showed consecutive reduction of its frequencies for the historic (1986–2005), mid-century (2046–2065) and end of the century (2081–2100) periods under the RCP4.5 and RCP8.5 scenarios. In general, our results with the largest reduction in cyclone numbers under the SSP5-8.5 scenario in the end of the century and similar responses under the SSP2-4.5 scenario in the middle and end of the 21st century are consistent with the trajectories of emissions in the SSPs, which are the highest to the end of the century for the SSP5-8.5 scenario and stabilizing at the middle of the century under the SSP5-4.5 scenario [78]. For example, earlier [15], using CMIP5 multimodel ensemble projection, analyzed future change of zonally averaged midlatitude storm tracks (derived from the filtered variance of the meridional wind component) over the Northern Hemisphere for the winter seasons and showed that the projected changes are close to each other under the RCP4.5 scenario at the middle and end of 21st century and under the RCP8.5 scenario at the mid-21st century, while the projected changes at the end of the 21st under the RCP8.5 scenario are almost twice as large as those projected for the mid-21st century.

3.3. Average cyclone tracks

The change in the local frequencies of cyclones over the Atlantic-European region may be associated, in addition to the change in the number of cyclogenesis events, with the shift of the main North Atlantic storm track from one latitude to another. Figure 8 shows the average position of cyclone tracks originating from the cyclogenesis areas (blue rectangles in Fig. 8) according to CMIP6 model simulations (see Fig. 2f, Fig. 4). To obtain average cyclone tracks for three previously selected 15-year periods, the average values of latitudes and longitudes of the selected cyclones were calculated at each time step (24 hours).

According to the Figure 8, average cyclone tracks from the Icelandic cyclogenesis area and the most southern one among tree North Atlantic cyclogenesis areas shift southward under SSP2-4.5 and SSP5-8.5 scenarios in the both periods of the middle and end of the century. Such southward shift is consistent with higher cyclone numbers projected for the British Isles, the North Sea and Baltic Sea. While cyclone tracks from the North Sea and Baltic Sea cyclogenesis areas are characterized by the comparable northward shift in the end of the 21st century under both scenarios. Over the Mediterranean Sea, the most substantial shift of the average cyclone track is expected under the SSP5-8.5 scenario: northward for the Western Mediterranean cyclogenesis area and southward for the both Eastern Mediterranean cyclogenesis areas. For the Black Sea cyclogenesis area, the most pronounced shift is northward in the middle of the 21st century under the SSP2-4.5 scenario. The northward shift of the Western Mediterranean cyclogenesis area is consistent with higher frequency of cyclones over Central Europe.

Preprints (www.preprints.org) | NOT PEER-REVIEWED | Posted: 27 July 2022 doi:10.20944/preprints202207.0417.v1

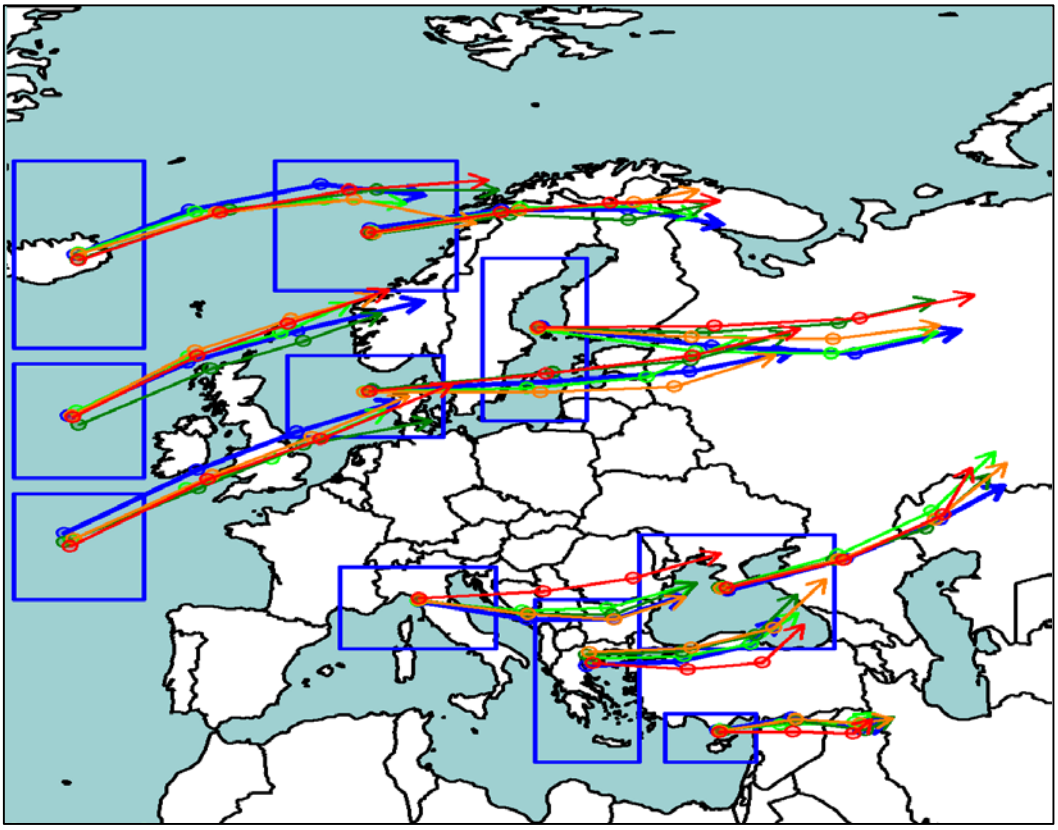

Figure 8. The average position of cyclone tracks originating from the cyclogenesis areas marked by blue rectangles. *Blue track* is for the period of the beginning of the century, *light green track* is for the mid-21st century under the SSP2-4.5 scenario, *green track* is for the end of the century under the SSP2-4.5 scenario, *orange track* is for the mid-21st century under the SSP5-8.5 scenario, *red track* is for the end of the century under the SSP5-8.5 scenario

4. Conclusions and Discussion

The following conclusions can be made based on the analysis of winter (DJF) cyclonic activity (frequency of cyclones, number of cyclogenesis events, number of cyclones and average cyclone tracks) in the Mediterranean-Black Sea region at the beginning (2000–2024), middle (1943–1957) and end (2086–2100) of the 21st century in the recent generation CMIP6 multimodel ensemble simulation under the scenarios of the intermediate (SSP2-4.5) and highest (SSP5-8.5) emissions.

In general, for the Atlantic-European region, it is shown that the recent historical (dated to the beginning of the century) spatial patterns of winter frequency of cyclones and the number of cyclogenesis events are apparently maintained in future, but most areas of the maximum cyclonic activity are projected to shrink and become noticeably weaker, especially to the end of the century and under the SSP5-8.5 scenario. Absolute anomalies of the future frequency of winter cyclones, relative to the recent historical period of the beginning of the century, show that there is a consistent among models decrease over the east of the Mediterranean Sea and north of Scandinavia, while there is an increase over the Central Europe and British Isles (due to the mostly January and December input), and the value of anomalies increases from the SSP2-4.5 to the SSP5-8.5 scenario.

This pattern is consistent with the dipole pattern shown in [5] using two domains (the British Isles and Iberia) and a tripolar pattern over Atlantic-European region mentioned, for example, in [6,23]. The reasons of the found pattern are likely related to a poleward shift of atmospheric rivers and moisture corridors [5], an extension of the North Atlantic storm track into Europe [23]. The North Atlantic storm track slightly weakens on its northern and southern flanks in association with the North Atlantic jet

 doi:10.20944/preprints202207.0417.v1

stream, which strengthens and extends further into Europe under the climate change conditions [28]. Generally, this tripolar pattern over the Atlantic European region is consistent with the broadening of the tropic and polar amplification of global warming in winter [10,11].

The area-averaged winter cyclone numbers (frequency of cyclones, number of cyclones and cyclogenesis events) over the western Mediterranean, eastern Mediterranean and the Black Sea subregions is not expected to show continuous reduction to the end of the century and from the SSP2-4.5 to the SSP5-8.5 scenario. Nevertheless, the largest drop of the median of all characteristics is expected for the end of the century under the SSP5-8.5 scenario, while the values in the middle of the 21st century under the same scenario are the highest among climate change responses. As for the SSP2-4.5 scenario, area-averaged cyclone numbers are projected to decrease in the middle of the century in the Eastern Mediterranean (especially in the frequency of cyclones) and the Black Sea subregions. Over the western Mediterranean subregion, there is an increase in the frequency of cyclones and decrease in the number of cyclogenesis events.

Such cyclone change responses in the Mediterranean-Black Sea subregions may be linked to the long-term (decadal–multidecadal) variability or regional features associated with averaging procedure. The behavior of different climate characteristics projected for the 21st century show considerable quasiperiodic long-term variability (interannual and decadal). These are, for example, frequency of the active storm track regions of the Northern Hemisphere [24], cyclone-related temperature and extreme precipitation over the Northern Hemisphere and in the Atlantic European region [3,8], storm frequency index over the North Atlantic [13], the integrated horizontal water vapor transport from the North Atlantic [5], the winter-time bandpass filtered mean SLP variance storm tracks over Western Europe [79], the frequency of intense Mediterranean cyclones for the extended winter period (October–March) [22]. However, generally researchers agree that these quasiperiodic anomalies are overwhelmed by the large changes projected for the 21st century [5] and anthropogenic forcing becomes dominant. As for the rare events such as the most intense cyclones, they do not show a consistent trend and may rather be attributed to long-term (e.g., decadal) variability than to the greenhouse gas forcing [22].

The average position of cyclone tracks originating from the cyclogenesis areas according to CMIP6 multimodel ensemble projection was found to be consistent with an increase of cyclonic activity in Central Europe due to a northward shift of the average track of the Western Mediterranean cyclogenesis area and southward shift of the of the average track of the North Atlantic cyclogenesis areas. Other cyclogenesis areas are characterized by a southward shift of the average track in the eastern Mediterranean region, and by a northward shift in the Black Sea region.

Such shifts of cyclone tracks were typical during the second part of the 20th and beginning of the 21st centuries [18,33] and generally occur as a result of a change in the North Atlantic oscillation phase due to a change in the intensity and position of the Iceland Low and the Azores High. In the 21st century, the positive NAO phase is expected to prevail [80], which is characterized by the shift of the North Atlantic storm track to Northern Europe and a decrease of cyclonic activity over the Mediterranean Sea. From this point of view, our results correspond to the strengthening of the NAO (transition to a positive phase), since under SSP2-4.5 scenario, our results show an increase in the frequency of cyclones in the winter months over Europe and a decrease in the Mediterranean region. However, the frequency of cyclones is expected to decrease also over Iceland, the Norwegian and the White Seas. The structure of the field of anomalies of the frequency of cyclones is more similar to the structure of the negative phase of the East Atlantic–West Russia pattern, which, as shown for the historical period in [81,82], corresponds to the circulation pattern opposite to the blocking in the following centers: the British Isles, Baltic region, northeast coast of the Mediterranean region, Black Sea region, southwest of Eastern Europe.

Thus, we have analyzed the changes in cyclonic activity in the Mediterranean-Black Sea region in the 21st century both in terms of cyclogenesis and the shift of cyclone tracks. In general, our study showed that the future winter cyclonic activity in the Mediterranean-Black Sea region responds unevenly to global climate changes, because regional and monthly features are important, as well as accounting for the long-term quasiperiodic variability. Our future research in this field we plan to devote to a more detailed study of the quantitative characteristics and causes of future cyclonic activity in the Mediterranean-Black Sea region using a regional model.

Author Contributions: All authors contributed to the study conception and design. Conceptualization, E.N.V.; methodology, A.S.L. and V.N.M.; software, V.Y.Z. and A.S.L.; validation, A.S.L. and V.Y.Z.; formal analysis, A.S.L. and V.Y.Z.; investigation, V.N.M. and A.S.L.; resources, A.S.L. and V.Y.Z.; data curation, A.S.L.; writing—original draft preparation, V.N.M. and A.S.L.; writing—review and editing, E.N.V.; visualization, A.S.L.; supervision, V.N.M.; project administration, E.N.V.; funding acquisition, E.N.V. All authors have read and agreed to the published version of the manuscript.

Funding: This research was funded by the state assignment of the Institute of Natural and Technical Systems, project reg. no. 121122300072–3.

Data Availability Statement: Cyclone identification and tracking programs are patented in the Unified Register of Russian Programs for Electronic Computers and Databases (certificates No. 2021662858 and No. 2021666926). Data supporting reported results are available on request.

Acknowledgments: We highly appreciate the free access to the datasets of CMIP6 (available online: https://esgf-data.dkrz.de/search/cmip6-dkrz/, accessed on 25 July 2022), NCEP/NCAR (available online: https://psl.noaa.gov/data/reanalysis/reanalysis.shtml, accessed on 25 July 2022) and ERA5 (available online: https://cds.climate.copernicus.eu/#!/search?text=ERA5&type=dataset, accessed on 25 July 2022) reanalyses.

Conflicts of Interest: The authors declare no conflict of interest.

References

1. Sinclair, V.A.; Rantanen, M.; Haapanala, P.; Räisänen, J.; Järvinen, H. The characteristics and structure of extra-tropical cyclones in a warmer climate. *Weather Clim. Dyn.* **2020**, *1*(1), 1–25. [https://doi.org/10.5194/wcd-1-1-2020]
2. Löptien, U.; Zolina, O.; Gulev, S.; Latif, M.; Soloviov, V. Cyclone life cycle characteristics over the Northern Hemisphere in coupled GCMs. *Clim. Dyn.* **2008**, *31*(5), 507–532. [https://doi.org/10.1007/s00382-007-0355-5]
3. Raible, C.C.; Pinto, J.G.; Ludwig, P.; Messmer, M. A review of past changes in extratropical cyclones in the northern hemisphere and what can be learned for the future. *Wiley Interdiscip. Rev. Clim. Change* **2021**, *12*(1), e680. [https://doi.org/10.1002/wcc.680]
4. Flaounas, E.; Davolio, S.; Raveh-Rubin, S.; Pantillon, F.; Miglietta, M.M.; Gaertner, M.A.; et al. Mediterranean cyclones: Current knowledge and open questions on dynamics, prediction, climatology and impacts. *Weather Clim. Dyn.* **2022**, *3*(1), 173–208. [https://doi.org/10.5194/wcd-3-173-2022]
5. Sousa, P.M.; Ramos, A.M.; Raible, C.C.; Messmer, M.; Tomé, R.; Pinto, J.G.; Trigo, R.M. North Atlantic integrated water vapor transport – From 850 to 2100 CE: Impacts on western European rainfall. *J. Clim.* **2020**, *33*(1), 263–279. [https://doi.org/10.1175/JCLI-D-19-0348.1]
6. Zappa, G.; Shaffrey, L.C.; Hodges, K.I.; Sansom, P.G.; Stephenson, D.B. A multimodel assessment of future projections of North Atlantic and European extratropical cyclones in the CMIP5 climate models. *J. Clim.* **2013**, *26*(16), 5846–5862. [https://doi.org/10.1175/JCLI-D-12-00573.1]
7. Yettella, V.; Kay, J.E. How will precipitation change in extratropical cyclones as the planet warms? Insights from a large initial condition climate model ensemble. *Clim. Dyn.* **2017**, *49*(5), 1765–1781. [https://doi.org/10.1007/s00382-016-3410-2]
8. Raible, C.C.; Messmer, M.; Lehner, F.; Stocker, T.F.; Blender, R. Extratropical cyclone statistics during the last millennium and the 21st century. *Clim. Past* **2018**, *14*(10), 1499–1514. [https://doi.org/10.5194/cp-14-1499-2018]
9. Hawcroft, M.; Walsh, E.; Hodges, K.; Zappa, G. Significantly increased extreme precipitation expected in Europe and North America from extratropical cyclones. *Environ. Res. Lett.* **2018**, *13*(12), 124006. [https://doi.org/10.1088/1748-9326/aaed59]
10. Zappa, G.; Shepherd, T.G. Storylines of atmospheric circulation change for European regional climate impact assessment. *J. Clim.* **2017**, *30*(16), 6561–6577. [https://doi.org/10.1175/JCLI-D-16-0807.1]
11. Hochman, A.; Alpert, P.; Kunin, P.; Rostkier-Edelstein, D.; Harpaz, T.; Saaroni, H.; Messori, G. The dynamics of cyclones in the twentyfirst century: the Eastern Mediterranean as an example. *Clim. Dyn.* **2020**, *54*(1), 561–574. [https://doi.org/10.1007/s00382-019-05017-3]

12. Seidel, D.J.; Fu, Q.; Randel, W.J.; Reichler, T.J. Widening of the tropical belt in a changing climate. *Nat. Geosci.* **2008**, *1*(1), 21–24. [https://doi.org/10.1038/ngeo.2007.38]
13. Fischer-Bruns, I.; Storch, H.V.; González-Rouco, J.F.; Zorita, E. Modelling the variability of midlatitude storm activity on decadal to century time scales. *Clim. Dyn.* **2005**, *25*(5), 461–476. [https://doi.org/10.1007/s00382-005-0036-1]
14. Harvey, B.J.; Shaffrey, L.C.; Woollings, T.J. Equator-topole temperature differences and the extra-tropical storm track responses of the CMIP5 climate models. *Clim. Dyn.* **2014**, *43*, 1171–1182. [https://doi.org/10.1007/s00382-013-1883-9]
15. Chang, E.K.; Guo, Y.; Xia, X. CMIP5 multimodel ensemble projection of storm track change under global warming. *J. Geophys. Res. Atmos.* **2012**, *117*, D23118. [https://doi.org/10.1029/2012JD018578]
16. Black, E.; Brayshaw, D.J.; Rambeau, C.M. Past, present and future precipitation in the Middle East: insights from models and observations. *Philos. Trans. Royal Soc. A* **2010**, *368*(1931), 5173–5184. [https://doi.org/10.1098/rsta.2010.0199]
17. Nissen, K.M.; Leckebusch, G.C; Pinto, J.G.; Renggli, D.; Ulbrich, S.; Ulbrich, U. Cyclones causing wind storms in the Mediterranean: characteristics, trends and links to large-scale patterns. *Nat. Hazards Earth Syst. Sci.* **2010**, *10*(7), 1379–1391. [https://doi.org/10.5194/nhess-10-1379-2010]
18. Voskresenskaya, E.N.; Maslova, V.N. Winter-spring cyclonic variability in the Mediterranean-Black Sea region associated with global processes in the ocean-atmosphere system. *Adv. Sci. Res.* **2011**, *6*(1), 237–243. [https://doi.org/10.5194/asr-6-237-2011]
19. Black, E. The influence of the North Atlantic Oscillation and European circulation regimes on the daily to interannual variability of winter precipitation in Israel. *Int. J. Climatol.* **2012**, *32*(11), 1654–1664. [https://doi.org/10.1002/joc.2383]
20. Maslova, V.N.; Voskresenskaya, E.N.; Lubkov, A.S.; Yurovsky; A.V. Temporal variability and predictability of intense cyclones in the Western and Eastern Mediterranean. *Atmosphere* **2021**, *12*(9), 1218. [https://doi.org/10.3390/atmos12091218]
21. Gagen, M.H.; Zorita, E.; McCarroll, D.; Zahn, M.; Young, G.H.; Robertson, I. North Atlantic summer storm tracks over Europe dominated by internal variability over the past millennium. *Nat. Geosci.* **2016**, *9*(8), 630–635. [https://doi.org/10.1038/NGEO2752]
22. Nissen, K.M.; Leckebusch, G.C.; Pinto, J.G.; Ulbrich, U. Mediterranean cyclones and windstorms in a changing climate. *Reg Environ Change* **2014**, *14*(5), 1873–1890. [https://doi.org/10.1007/s10113-012-0400-8]
23. Priestley, M.D.; Catto, J.L. Future changes in the extratropical storm tracks and cyclone intensity, wind speed, and structure. *Weather Clim. Dyn.* **2022**, *3*(1), 337–360. [https://doi.org/10.5194/wcd-3-337-2022]
24. Eichler, T.P.; Gaggini, N.; Pan, Z. Impacts of global warming on Northern Hemisphere winter storm tracks in the CMIP5 model suite. *J. Geophys. Res. Atmos.* **2013**, *118*(10), 3919–3932. [https://doi.org/10.1002/jgrd.50286]
25. Ulbrich, U.; Leckebusch, G.C.; Pinto, J.G. Extra-tropical cyclones in the present and future climate: a review. *Theor. Appl. Climatol.* **2009**, *96*(1), 117–131. [https://doi.org/10.1007/s00704-008-0083-8]
26. Feser, F.; Barcikowska, M.; Krueger, O.; Schenk, F.; Weisse, R.; Xia, L. Storminess over the North Atlantic and northwestern Europe – A review. *Q. J. R. Meteorol. Soc.* **2015**, *141*(687), 350–382. [https://doi.org/10.1002/qj.2364]
27. Michaelis, A.C.; Willison, J.; Lackmann, G.M.; Robinson, W.A. Changes in winter North Atlantic extratropical cyclones in high-resolution regional pseudo–global warming simulations. *J. Clim.* **2017**, *30*(17), 6905–6925. [https://doi.org/10.1175/JCLI-D-16-0697.1]
28. Harvey, B.J.; Cook, P.; Shaffrey, L.C.; Schiemann, R. The response of the northern hemisphere storm tracks and jet streams to climate change in the CMIP3, CMIP5, and CMIP6 climate models. *J. Geophys. Res. Atmos.* **2020**, *125*(23), e2020JD032701. [https://doi.org/10.1029/2020JD032701]
29. Lionello, P.; Dalan, F.; Elvini, E. Cyclones in the Mediterranean region: The present and the doubled CO2 climate scenarios. *Climate Res.* **2002**, *22*, 147–159. [https://doi.org/10.3354/cr022147]
30. Zappa, G.; Hawcroft, M.K.; Shaffrey, L.; Black, E.; Brayshaw, D.J. Extratropical cyclones and the projected decline of winter Mediterranean precipitation in the CMIP5 models. *Clim. Dyn.* **2015**, *45*(7), 1727–1738. [https://doi.org/10.1007/s00382-014-2426-8]
31. Trigo, I.F.; Davies, T.D.; Bigg, G.R. Decline in Mediterranean rainfall caused by weakening of Mediterranean cyclones. *Geophys. Res. Lett.* **2000**, *27*, 2913–2916. [https://doi.org/10.1029/2000GL011526]
32. Flocas, H.A.; Simmonds, I.; Kouroutzoglou, J.; Keay, K.; Hatzaki, M.; Bricolas, V.; Asimakopoulos, D. On cyclonic tracks over the Eastern Mediterranean. *J. Climate* **2010**, *23*, 5243–5257. [https://doi.org/10.1175/2010JCLI3426.1]
33. Maslova, V.N.; Voskresenskaya, E.N.; Lubkov, A.S.; Yurovsky, A.V.; Zhuravskiy, V.Y.; Evstigneev, V.P. Intense cyclones in the Black Sea region: change, variability, predictability and manifestations in the storm activity. *Sustainability* **2020**, *12*(11), 4468. [https://doi.org/10.3390/su12114468]
34. Enzel, Y.; Bookman, R.; Sharon, D.; Gvirtzman, H.; Dayan, U.; Ziv, B.; Stein, M. Late Holocene climates of the Near East deduced from Dead Sea level variations and modern regional winter rainfall. *Quat. Res.* **2003**, *60*(3), 263–273. [https://doi.org/10.1016/j.yqres.2003.07.011]
35. Reale, M.; Cabos Narvaez, W.D.; Cavicchia, L.; Conte, D.; Coppola, E.; Flaounas, E.; et al. Future projections of Mediterranean cyclone characteristics using the Med-CORDEX ensemble of coupled regional climate system models. *Clim. Dyn.* **2022**, *58*(9), 2501–2524. [https://doi.org/10.1007/s00382-021-06018-x]
36. Lionello, P.; Giorgi, F. Winter precipitation and cyclones in the Mediterranean region: future climate scenarios in a regional simulation. *Adv. Geosci.* **2007**, *12*, 153–158. [https://doi.org/10.5194/adgeo-12-153-2007]
37. Peleg, N.; Bartov, M.; Morin, E. CMIP5-predicted climate shifts over the East Mediterranean: implications for the transition region between Mediterranean and semi-arid climates. *Int. J. Climatol.* **2015**, *35*(8), 2144–2153. [https://doi.org/10.1002/joc.4114]

38. Hochman, A.; Harpaz, T.; Saaroni, H.; Alpert, P. Synoptic classification in 21st century CMIP5 predictions over the Eastern Mediterranean with focus on cyclones. *Int. J. Climatol.* **2018**, *38*(3), 1476–1483. [https://doi.org/10.1002/joc.5260]
39. Sinclair, M.R. An objective cyclone climatology for the Southern Hemisphere. *Mon. Wea. Rev.* **1994**, *122*, 2239–2256. [https://doi.org/10.1175/1520-0493(1994)122<2239:AOCCFT>2.0.CO;2]
40. Sinclair, M.R. Objective identification of cyclones and their circulation intensity, and climatology. *Wea. Forecasting* **1997**, *12*, 591–608. [https://doi.org/10.1175/1520-0434(1997)012<0595:OIOCAT>2.0.CO;2]
41. Serreze, M.C. Climatological aspects of cyclone development and decay in the Arctic. *Atmos.–Ocean* **1995**, *33*, 1–23. [https://doi.org/10.1080/07055900.1995.9649522]
42. Simmonds, I.; Burke, C.; Keay, K. Arctic climate change as manifest in cyclone behavior. *J. Climate* **2008**, *21*, 5777–5796. [https://doi.org/10.1175/2008JCLI2366.1]
43. Pinto, J.G.; Spangehl, T.; Ulbrich, U.; Speth, P. Sensitivities of a cyclone detection and tracking algorithm: Individual tracks and climatology. *Meteor. Z.* **2005**, *14*, 823–838. [https://doi.org/10.1127/0941-2948/2005/0068]
44. Raible, C.C.; Della-Marta, P.M.; Schwierz, C.; Wernli, H.; Blender, R. Northern Hemisphere extratropical cyclones: A comparison of detection and tracking methods and different reanalyses. *Mon. Wea. Rev.* **2008**, *136*, 880–897. [https://doi.org/10.1175/2007MWR2143.1]
45. Hodges, K.I.; Hoskins, B.J.; Boyle, J.; Thorncroft, C. A comparison of recent reanalysis datasets using objective feature tracking: Storm tracks and tropical easterly waves. *Mon. Wea. Rev.* **2003**, *131*, 2012–2037. [https://doi.org/10.1175/1520-0493(2003)131<2012:ACORRD>2.0.CO;2]
46. Bardin, M.Yu.; Polonsky, A.B. North Atlantic oscillation and synoptic variability in the European-Atlantic region in winter. *Izv. Atmos. Oceanic Phys.* **2005**, *41*, 127–136.
47. Wang, X.L.; Swail, V.R.; Zwiers, F.W. Climatology and changes of extratropical cyclone activity: Comparison of ERA-40 with NCEP/NCAR reanalysis for 1958–2001. *J. Climate* **2006**, *19*, 3145–3166. [https://doi.org/10.1175/JCLI3781.1]
48. Rudeva, I.; Gulev, S.K. Climatology of cyclone size characteristics and their changes during the cyclone life cycle. *Mon. Wea. Rev.* **2007**, *135*, 2568–2587. [https://doi.org/10.1175/MWR3420.1]
49. Zhuravsky, V.Y.; Voskresenskaya, E.N. Technology of cyclones sepaparion from global reanalyes data seta on meteorological fields. *Monit. Syst. Environ.* **2018**, *1*, 74–78. [https://doi.org/10.33075/2220-5861-2018-1-74-78]
50. Grist, J.P.; Josey, S.A.; Sinha, B.; Catto, J.L.; Roberts, M.J.; Coward, A.C. Future evolution of an eddy rich ocean associated with enhanced East Atlantic storminess in a coupled model projection. *Geophys. Res. Lett.* **2021**, *48*, e2021GL092719. [https://doi.org/10.1029/2021GL092719]
51. Muskulus, M.; Jacob, D. Tracking cyclones in regional model data: the future of Mediterranean storms. *Adv. Geosci.* **2005**, *2*, 13–19. [https://doi.org/10.5194/adgeo-2-13-2005]
52. Meehl, G.A.; Boer, G.J.; Covey, C.; Latif, M.; Stouffer, R.J. The coupled model intercomparison project (CMIP). *Bull. Am. Meteorol. Soc.* **2000**, *81*(2), 313–318.
53. Meehl, G.A.; Covey, C.; McAvaney, B.; Latif, M.; Stouffer, R.J. Overview of the coupled model intercomparison project. *Bull. Am. Meteorol. Soc.* **2005**, *86*(1), 89–93. [https://doi.org/10.1175/BAMS-86-1-89]
54. Eyring, V.; Bony, S.; Meehl, G.A.; Senior, C.A.; Stevens, B.; Stouffer, R.J.; Taylor, K.E. Overview of the Coupled Model Intercomparison Project Phase 6 (CMIP6) experimental design and organization. *Geosci. Model Dev.* **2016**, *9*(5), 1937–1958. [https://doi.org/10.5194/gmd-9-1937-2016]
55. Priestley, M.D.; Ackerley, D.; Catto, J.L.; Hodges, K.I.; McDonald, R.E.; Lee, R.W. An overview of the extratropical storm tracks in CMIP6 historical simulations. *J. Clim.* **2020**, *33*(15), 6315–6343. [https://doi.org/10.1175/JCLI-D-19-0928.1]
56. Fernandez-Granja, J.A.; Casanueva, A.; Bedia, J.; Fernandez, J. Improved atmospheric circulation over Europe by the new generation of CMIP6 earth system models. *Clim. Dyn.* **2021**, *56*(11), 3527–3540. [https://doi.org/10.1007/s00382-021-05652-9]
57. Zappa, G.; Shaffrey, L.C.; Hodges, K.I. The ability of CMIP5 models to simulate North Atlantic extratropical cyclones. *J. Clim.* **2013**, *26*(15), 5379–5396. [https://doi.org/10.1175/JCLI-D-12-00501.1]
58. Akperov, M.; Rinke, A.; Mokhov, I.I.; Semenov, V.A.; Parfenova, M.R.; Matthes, H.; et al. Future projections of cyclone activity in the Arctic for the 21st century from regional climate models (Arctic-CORDEX). *Glob. Planet. Change* **2019**, *182*, 103005. [https://doi.org/10.1016/j.gloplacha.2019.103005]
59. Cherchi, A.; Fogli, P.G.; Lovato, T.; Peano, D.; Iovino, D.; Gualdi, S.; et al. Global mean climate and main patterns of variability in the CMCC-CM2 coupled model. *J. Adv. Model.* **2018**, *11*, 185–209. [https://doi.org/10.1029/2018MS001369]
60. Lovato, T.; Peano, D.; Butenschön, M.; Materia, S.; Iovino, D.; Scoccimarro, E.; et al. CMIP6 simulations with the CMCC Earth System Model (CMCC-ESM2). *J. Adv. Model.* **2022**, *14*(3), e2021MS002814. [https://doi.org/10.1029/2021MS002814]
61. Boucher, O.; Servonnat, J.; Albright, A.L.; Aumont, O.; Balkanski, Y.; Bastrikov, V.; et al. Presentation and evaluation of the IPSL-CM6A-LR climate model. *J. Adv. Model.* **2020**, *12*, e2019MS002010. [https://doi.org/10.1029/2019MS002010]
62. Müller, W.A.; Jungclaus, J.H.; Mauritsen, T.; Baehr, J.; Bittner, M.; Budich, R.; et al. A higher-resolution version of the Max Planck Institute Earth System Model (MPI-ESM1.2-HR). *J. Adv. Model* **2018**, *10*, 1383–1413. [https://doi.org/10.1029/2017MS001217]
63. Mauritsen, T.; Bader, J.; Becker, T.; Behrens, J.; Bittner, M.; Brokopf, R.; et al. Developments in the MPI-M Earth System Model version 1.2 (MPI-ESM1.2) and its response to increasing CO2. *J. Adv. Model* **2019**, *11*, 998–1038. [https://doi.org/10.1029/2018MS001400]

64. Seland, Ø.; Bentsen, M.; Olivié, D.; Toniazzo, T.; Gjermundsen, A.; Graff, L.S.; et al. Overview of the Norwegian Earth System Model (NorESM2) and key climate response of CMIP6 DECK, historical, and scenario simulations. *Geosci. Model Dev.* **2020**, *13*(12), 6165–6200. [https://doi.org/10.5194/gmd-13-6165-2020]
65. Lee, W.-L.; Wang, Y.-C.; Shiu, C.-J.; Tsai, I.; Tu, C.-Y.; Lan, Y.-Y.; et al. Taiwan Earth System Model: Description and evaluation of mean. *Geosci. Model Dev.* **2020**, *13*, 3887–3904. [https://doi.org/10.5194/gmd-2019-377]
66. *IPCC SRES: Special report on emissions scenarios*: *A special report of Working Group III of the Intergovernmental Panel on Climate Change*; Nakićenović, N., Swart, R., Eds.; Cambridge University Press, 2000.
67. *IPCC TAR WG3: Climate change 2001: mitigation: contribution of Working Group III to the third assessment report of the Intergovernmental Panel on Climate Change*; Metz, B., Davidson, O., Swart, R., Pan, J., Eds.; Cambridge University Press, 2001; Volume 3.
68. *IPCC AR4 SYR: Synthesis Report, Contribution of Working Groups I, II and III to the Fourth Assessment Report of the Intergovernmental Panel on Climate Change*; Pachauri, R.K., Reisinger, A., et al., Eds.; IPCC, 2007.
69. *IPCC AR5 WG1: Climate Change. The Physical Science Basis. Working Group 1 (WG1) Contribution to the Intergovernmental Panel on Climate Change (IPCC) 5th Assessment Report (AR5)*; Stocker, T.F., et al., Eds.; Cambridge University Press, 2013.
70. *IPCC, 2021: Climate Change. The Physical Science Basis. Contribution of Working Group I to the Sixth Assessment Report of the Intergovernmental Panel on Climate Change*; Masson-Delmotte, V., Zhai P.; Pirani, A., et al., Eds.; Cambridge University Press, 2021.
71. Hausfather, Z.; Peters, G.P. Emissions – the 'business as usual' story is misleading. *Nature* **2020**, *577*, 618–620. [https://doi.org/10.1038/d41586-020-00177-3]
72. Pekarnikova, M.; Polonsky, A. Anthropogenic climate change and international-juridical activity on climate mitigation. Part 2. Implementation of climate legal acts at the present stage and their prospects. *Gos. pravo (Mosk.)* **2021**, *5*, 118–124. [https://doi.org/10.31857/S102694520012784-3]
73. Polonsky, A.; Pekarnikova, M.E. Anthropogenic climate change and international-juridical activity on climate mitigation. Part 1. From the UN Framework Convention to the Paris Agreement. *Gos. pravo (Mosk.)* **2021**, *4*, 104–113. [https://doi.org/10.31857/S102694520012719-1]
74. Kalnay, E.; Kanamitsu, M.; Kistler, R.; Collins, W.; Deaven, D.; Gandin, L.; et al. The NCEP/NCAR 40-year reanalysis project. *Bull. Am. Meteorol. Soc.* **1996**, *77*(3), 437–472. [https://doi.org/10.1175/1520-0477(1996)077<0437:TNYRP>2.0.CO;2]
75. Hersbach, H.; Bell, B.; Berrisford, P.; Hirahara, S.; Horányi, A.; Muñoz-Sabater, J.; et al. The ERA5 global reanalysis. *Q. J. R. Meteorol. Soc.* **2020**, *146*(730), 1999–2049. [https://doi.org/10.1002/qj.3803]
76. Khromov, S.P.; Petrosyants, M.A. *Meteorology and climatology*, 5th ed.; MSU: Moscow, Russia, 2001; 528 p.
77. Ziv, B.; Harpaz, T.; Saaroni, H.; Blender, R. A new methodology for identifying daughter cyclogenesis: application for the Mediterranean Basin. *Int. J. Climatol.* **2015**, *35*(13), 3847–3861. [https://doi.org/10.1002/joc.4250]
78. Riahi, K.; van Vuuren, D.P.; Kriegler, E.; Edmonds, J.; O'Neill, B.C.; Fujimori, S.; et al. The shared socioeconomic pathways and their energy, land use, and greenhouse gas emissions implications: an overview. *Glob. Environ. Change,* **2017**, *42*, 153–168. [https://doi.org/10.1016/j.gloenvcha.2016.05.009]
79. Harvey, B.J.; Shaffrey, L.C.; Woollings, T.J.; Zappa, G.; Hodges, K.I. How large are projected 21st century storm track changes? *Geophys. Res. Lett.* **2012**, *39*(18), L18707. [https://doi.org/10.1029/2012GL052873]
80. Pinto, J.G.; Ulbrich, U.; Leckebusch, G.C.; Spangehl, T; Reyers, M; Zacharias, S. Changes in storm track and cyclone activity in three SRES ensemble experiments with the ECHAM5/MPI-OM1 GCM. *Clim. Dyn.* **2007**, *29*, 195–210. [https://doi.org/10.1007/s00382-007-0230-4]
81. Bardin, M.Yu.; Platova, T.V.; Samokhina, O.F. Specific features of variability of cyclone activity in northern extratropics associated with leading atmospheric circulation modes in Atlantic-European sector. *Fundam Appl. Climatol.* **2015**, *2*, 14–40.
82. Maslova, V.; Voskresenskaya, E.; Yurovsky, A.; Bardin, M. Winter cyclone regimes over the North Atlantic region. *Theor. Appl. Climatol.* **2022,** *148*(3), 1689–1711. [https://doi.org/10.1007/s00704-022-04018-3]